

The radiation tolerance of specific optical fibres exposed to 650 kGy(Si) of ionizing radiation

This article has been downloaded from IOPscience. Please scroll down to see the full text article.

2009 JINST 4 P07010

(<http://iopscience.iop.org/1748-0221/4/07/P07010>)

The Table of Contents and more related content is available

Download details:

IP Address: 129.119.200.41

The article was downloaded on 27/07/2009 at 19:23

Please note that terms and conditions apply.

The radiation tolerance of specific optical fibres exposed to 650 kGy(Si) of ionizing radiation

B. Arvidsson,^d K. Dunn,^e C. Issever,^e B.T. Huffman,^{e,1} M. Jones,^e J. Kierstead,^a G. Kuyt,^b T. Liu,^f A. Povey,^e E. Regnier,^c A.R. Weidberg,^e A. Xiang^f and J. Ye^f

^aBrookhaven National Laboratory, Physics Department,
Bldg. 510A, Upton, NY 11973, U.S.A.

^bDraka,
P.O. Box 75979, 1070 AZ Amsterdam, Netherlands

^cDraka Communications, Site Date 4,
Batiment DO, Routes de Nozay, 94160 Marcoussis, France

^dEricsson Network Technologies AB,
Kabelv 1, SE-82482 Hudiksvall, Sweden

^ePhysics Department, University of Oxford,
Keble Road, Oxford OX1 3RH, U.K.

^fPhysics Department, Southern Methodist University,
106 Fondren Science Building, Dallas, TX 75275-0175, U.S.A.

E-mail: t.huffman1@physics.ox.ac.uk

ABSTRACT: The LHC upgrade will extensively increase the area of silicon detectors used in the ATLAS experiment and require substantial changes to the readout system of both the ATLAS and CMS experiments. The two experiments are expected to use optical systems for part of the data and control paths which must withstand levels of radiation equivalent to a dose of approximately 400 kGy(Si) at 30 cm from the collision region (including a safety factor of 1.5). As part of the search for acceptably radiation hard optical fibres, four Graded Index multimode (GRIN) optical fibres and one single-mode (SM) fibre were tested to 650 kGy(Si) equivalent dose. One of the GRIN fibres was also tested at 5 different dose rates, in order to understand the dose rate effects. These tests have validated the radiation tolerance of a single-mode fibre and two multimode fibres for use at the SLHC for warm operation. Some interesting features of the time dependence of the fibre radiation damage and future plans are discussed.

KEYWORDS: Optical detector readout concepts; Radiation calculations

¹Corresponding author.

Contents

1	Introduction	1
2	SLHC upgrade and the radiation environment	2
3	Fibre radiation tolerance	2
3.1	Fibres used	5
4	Experimental configuration	5
4.1	The radiation facility, SCK-CEN	6
4.2	The radiation facility at BNL	9
4.3	The experimental configuration	10
4.3.1	The Brigitte (high dose rate) experiment	11
4.3.2	The Rita (low dose rate) experiment	12
4.3.3	The BNL experiment	12
4.3.4	Stability tests and experimental accuracy	12
4.3.5	Further discussion of the stability of the multimode system	14
5	Test results	15
5.1	High dose results — Brigitte	15
5.2	Intermediate dose rate results — Rita	15
5.3	Low dose rate results BNL	15
5.4	Combined results	16
5.4.1	Route specific RIA	16
5.5	The early attenuation spike	19
5.6	Future plans	24
6	Conclusions	24
A	RIA fits functions	25

1 Introduction

Fibre optic links are widely used in the current generation of Large Hadron Collider (LHC) experiments. They will also be used for the upgraded detectors at the Super-LHC (SLHC). It is therefore essential to identify suitably radiation tolerant fibres for the higher doses expected at SLHC. The radiation doses expected at SLHC will be described in section 2. A brief review of theory and experiments on fibre radiation tolerance and the properties of the fibres used in this study will be summarised in section 3. Three different radiation facilities were used in these studies in order to

understand dose rate effects. These facilities and the experimental procedures will be described in section 4. The results from the different facilities will first be described individually and then the data will be combined in order to understand the dose rate effects in section 5. Evidence for strong temperature dependent effects was found and this will be discussed in section 5.5. The outlook for further research will also be discussed. Some conclusions will be given in section 6.

2 SLHC upgrade and the radiation environment

The SLHC programme aims to increase the integrated luminosity by a factor of 10 compared to that expected for the LHC [1]. The LHC studies were based on the assumption that the integrated luminosity available for physics would be 300 fb^{-1} . Therefore the SLHC studies [2] are based on the assumption that the integrated luminosity delivered will be 3000 fb^{-1} . Detailed calculations of the radiation doses expected for the upgraded ATLAS and CMS detectors at SLHC are under way but since these results are not yet available, this study uses a simple scaling of the radiation levels already calculated for ATLAS [4] based on the ratio of integrated luminosities expected. Since the fibre radiation damage is most sensitive to the ionising dose (see section 3), this is expected to be a good approximation [3]. In the highest dose location considered for the fibres in the upgraded ATLAS inner detector, this would result in a total dose of $\sim 250 \text{ kGy(Si)}$ (at a radius of 30 cm from the beam line) before allowing for any additional safety factors. The effects of these safety factors are discussed in section 5.4.1.

The map of the ionising dose expected for ATLAS [4] is shown in figure 1. Although the region closest to the beam line has the highest dose, there will be longer lengths of fibres further out which will see lower doses. The predicted effect of radiation damage on the fibres is calculated by combining the expected doses with the measured radiation induced absorption for a given assumption about the fibre routing (see section 5.2). While the 2D radiation map gives a qualitative understanding of the complex radiation field, a more quantitative assessment is given in figure 2 which shows the expected dose as a function of radius (R) from the beam line for 1 year of LHC operation, for several slices in the distance along the beam line from the centre of the detector (z).

3 Fibre radiation tolerance

Ionising radiation can create defects in the glass which lead to new energy levels in the glass and these can result in an increase in absorption at the relevant wavelengths [5]. High energy particles like neutrons do cause an increase in absorption but this is mainly due to the ionisation effects from secondary particles. At the extremely high neutron fluences for fission and fusion reactors ($\sim 10^{18} \text{ n/cm}^2$), the neutron knock-on produce recoil protons which can result in growth of the OH vibration band [6]. However, these effects are not expected to be important for the (~ 3 orders of magnitude) lower fluences expected at SLHC. Some evidence that the neutron induced damage scales with the resulting ionizing dose is given in [7] and [9]. Therefore, this study only considers the effects of ionising radiation.

There are many factors which influence the radiation tolerance of optical fibres. The most important of these are the level and type of dopants and impurities present in the core, the details of the fibre drawing process, the wavelength of operation and the environmental conditions in which

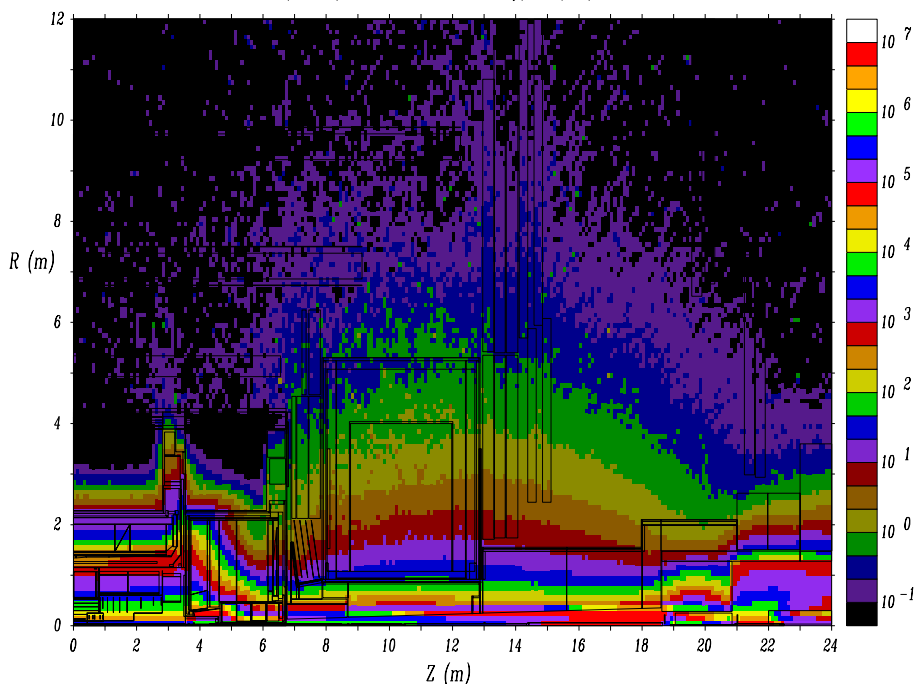


Figure 1. Radiation map showing the expected ionising dose (Gy) as a function of radius from the beam line (R) and distance along the beam line from the centre of the detector (z) for 1 year of operation at the nominal LHC luminosity of $10^{34} \text{ cm}^{-2} \text{ s}^{-1}$.

the fibre is exposed to radiation. The presence of very small quantities of impurities can significantly degrade the radiation tolerance of the fibre. Many commercial multimode fibres contain phosphorous in the core because it lowers the temperature required for deposition during the pre-form manufacture. This implies a lower humidity in the process and hence results in lower OH content in the fibre. It is well known that the presence of phosphorous leads to stable defects which cause large increases in the radiation induced absorption (RIA), see for example [7]. The presence of alkaline and metal impurities can also lead to a significant increase in RIA. The details of the fibre drawing process determines the number of defects created which can significantly affect the RIA of the fibre. The presence of water in the fibre manufacturing process leads to some OH content in fibre. Higher OH content fibre can have larger RIA for wavelengths around 600 nm but this effect should not be so significant at longer wavelengths [5]. In addition, current commercial telecom fibres all have very low OH concentrations in the fibre core (≤ 1 ppb) in order to have as flat as possible attenuation spectrum between 1310 nm and 1510 nm.

In general, telecom fibres are drawn at very high speeds (typically of the order of 1 km/minute) and the fibres are exposed to extremely rapid temperature changes ($\sim 2000^\circ\text{C/s}$). This can result in the creation of defects in the SiO_2 structure and the weakening of bonds, which can significantly affect the RIA of the fibre. Therefore radiation tolerant fibres generally require specific drawing conditions with an improved thermal control [8].

The wavelengths considered in this paper for data transmission in optical fibres are 850 nm and 1310 nm. The silica defects created under irradiation have electronic transitions in the UV-visible range. The resulting RIA therefore peaks at lower wavelengths, which implies that the radiation tolerance of the fibres is expected to be better at 1310 nm than at 850 nm.

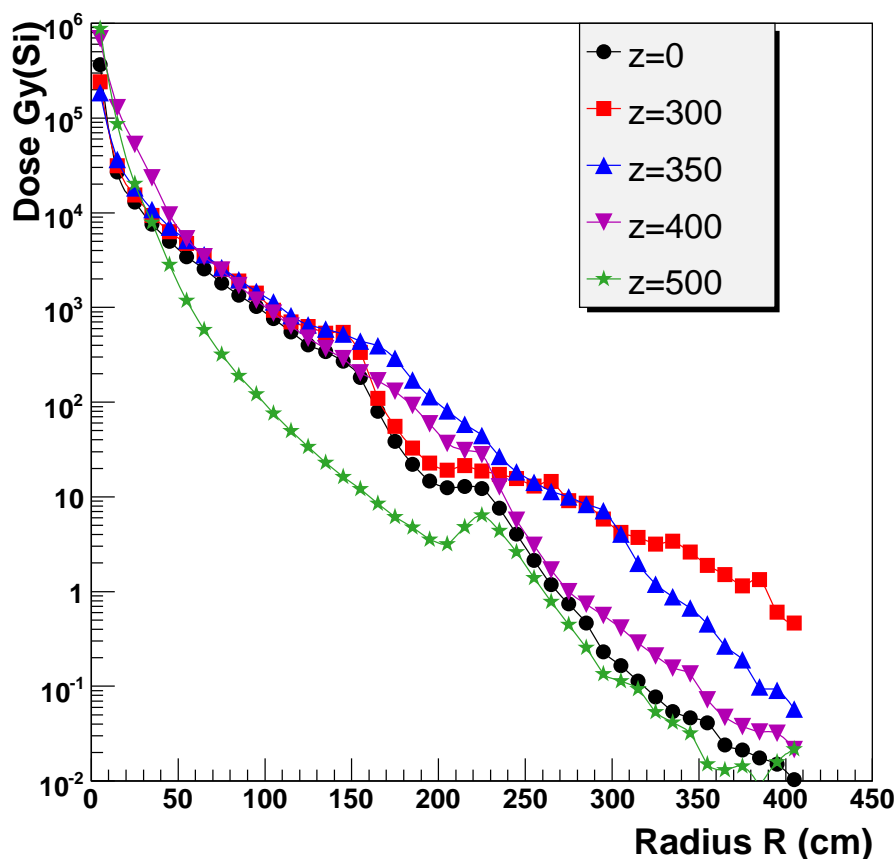


Figure 2. Radiation map showing the expected ionising dose (Gy) as a function of radius from the beam line (R) for 5 different distances along the beam line from the centre of the detector (z) for 1 year of operation at the nominal LHC luminosity of $10^{34} \text{ cm}^{-2} \text{ s}^{-1}$.

Some of the defects caused by radiation can anneal with time [10], [5]. The rate of the annealing depends on the reaction kinetics [11], [5] and is therefore very sensitive to temperature with faster annealing expected at higher temperatures. High optical power in the fibre during radiation can also accelerate the annealing by the so-called photo-bleaching process [10]. The actual RIA for a particular fibre type, that will result from a given radiation exposure depends critically on the conditions used, namely the temperature, the dose rate and the level of optical power as well as the total dose received.

The complexity of the factors that influence RIA make reliable predictions of the radiation tolerance for a particular fibre difficult. While it is easy to determine that some fibres will be sensitive to RIA, it is very difficult to predict that a particular fibre will be radiation tolerant. Thus radiation testing is essential to validate the radiation tolerance of any particular fibre. Ideally this testing should be carried out in an environment which simulates the final application but for the case of SLHC operation it is obviously not practical to simulate the full dose at the correct dose rate as this would take many years. However, from comparisons of data from radiation tests with identical conditions apart from dose rates, it is in principle possible to predict the RIA that would be expected at the dose rate in the final application.

3.1 Fibres used

The optical links for ATLAS and CMS are expected to operate at speeds in the range 5–10 Gbits/s for distances of up to 150 m. Therefore the required fibre bandwidth is $\sim 1000 \text{ MHz} \cdot \text{km}$. The developers of optical data links for the SLHC are considering the use of 850 nm or 1310 nm wavelengths. The final choice of wavelengths will depend on the radiation tolerance of the laser emitters and *p-i-n* photodiodes as well as the fibres. This implies that suitable radiation tolerant multimode fibres for use at 850 nm and single-mode fibres for use at 1310 nm need to be identified.

An extremely radiation tolerant single-mode fibre was developed for use in the LHC machine [9] and this fibre would be sufficiently radiation tolerant for use inside a tracking detector at SLHC.

The CMS experiment has a very large installed fibre plant and it would therefore be an attractive option to continue to use this for the SLHC. Extensive testing of the fibres used for CMS showed that a telecoms single-mode fibre, SMF-28,¹ would be sufficiently radiation tolerant for use at the LHC [12]. Some limited testing of this fibre indicated that it might be sufficiently radiation tolerant for use at the SLHC [13] but further radiation testing is required to validate this.

A very radiation tolerant pure silica core Step Index Multi Mode (SIMM) fibre was used by the ATLAS SemiConductor Tracker and Pixel detectors [7]. Tests of this fibre up to SLHC doses indicated that it would probably be suitably radiation tolerant for use at the SLHC. However, because of its SIMM structure, it has a relatively low bandwidth which makes it unsuitable for SLHC applications which will require very high bandwidth fibres.

Therefore, this study will look at candidates for suitably radiation tolerant Graded Index Multimode fibres (GRIN) with high bandwidths (for operation at 850 nm) and one single-mode fibre (for operation at 1310 nm). One multimode fibre candidate considered is the Infinicor SX+² fibre because it is known to have no phosphorous in the core. Another multimode fibre considered is a commercial fibre produced by Draka.³ Two other multimode fibres were studied which are prototypes produced by Draka in collaboration with Ericsson,⁴ who are developing radiation tolerant fibres for other applications. None of the fibres used in this study contained phosphorous in the core. The Draka RHP-1 contains F dopant in the core and the cladding to create the required refractive index profile, whereas all the other fibres used in this study contain Ge dopant in the core.

Some key parameters for these fibres are given in table 1 and table 2. The dispersion for the Single Mode fibre is defined in terms of the zero dispersion wavelength (λ_0) and the zero dispersion slope (S_0) as

$$D(\lambda) = (S_0/4) \left(\lambda - (\lambda_0)^4 / \lambda^3 \right) \quad (3.1)$$

4 Experimental configuration

All the radiation tests used ^{60}Co radioactive sources. Different strength sources were used to study the dose rate dependent effects for one of the multimode fibres. In this section we discuss the de-

¹Corning, http://www.corning.com/opticalfiber/products/infinicor_fibers.aspx.

²Corning, <http://www.corning.com/WorkArea/showcontent.aspx?id=15485>.

³Draka, <http://www.drakafibre.com>.

⁴Ericsson, <http://www.ericsson.com/>.

Table 1. Parameters of the SMF-28 single-mode fibre used in this study.

Wavelength (nm)	Core diameter (μm)	Numerical Aperture	λ_0 Dispersion minimum (nm)	S_0 Dispersion slope (ps/(nm.km))	Attenuation (dB/km)
1310	8.2	0.14	1302–1322	< 0.09	< 0.34

Table 2. Parameters of the multimode fibres used in this study.

Fibre	Wavelength (nm)	Core diameter (μm)	Numerical Aperture	Bandwidth (MHz.km)	Attenuation (dB/km)
Infincor SX+	850	50 ± 2.5	0.200 ± 0.015	> 2000	< 2.3
Draka-1	850	50 ± 2	0.200 ± 0.015	820	< 2.5
Draka-RHP-1	850	50 ± 2	0.200 ± 0.015	To be optimised	< 2.0
Draka RHP-2	850	50 ± 4	0.200 ± 0.015	To be optimised	< 2.0

Table 3. Dose rates, total doses and fibres used for the different exposures. VCSEL refers to Vertical Cavity Surface Emitting Laser and EEL to Edge Emitting Laser.

Source	Dose Rate kGy(Si)/hour	Total Dose kGy(Si)	Fibres exposed	Length (m)	Single Mode (SM) or Multimode (MM)	Light source
Brigitte	22.5	650	Infincor SX+	50	MM	VCSEL
Brigitte	22.5	650	Draka-1	50	MM	VCSEL
Brigitte	22.5	650	Draka-RHP-1	50	MM	VCSEL
Brigitte	22.5	650	Draka RHP-2	50	MM	VCSEL
Brigitte	22.5	650	SMF-28	50	SM	EEL
Rita	1.01	67	Infincor SX+	50	MM	VCSEL
Rita	1.01	67	Infincor SX+	50	MM	LED
BNL	0.424	18.2	Infincor SX+	30	MM	VCSEL
BNL	0.343	14.8	Infincor SX+	80	MM	VCSEL
BNL	0.0265	1.14	Infincor SX+	180	MM	VCSEL

tails of the sources at the two experimental sites: SCK-CEN⁵ and Brookhaven National Laboratory (BNL).⁶ We then describe how the experiments were done and tests of the stability of the experiments so that we can set an estimate of the uncertainty in our final RIA results. The different dose rates used and the total doses are summarised in table 3.

4.1 The radiation facility, SCK-CEN

The SCK-CEN facility is located near Mol, Belgium. There are several test reactors and exposure areas on this site. However, for our particular tests two ⁶⁰Co gamma ray sources were used. The high dose source is called “Brigitte” and delivered 22.5 kGy(Si)/hr maximum dose through a volume 10 cm in height and 22 cm in diameter. The low dose source is called “Rita” and delivered

⁵SCK-CEN, Belgium Nuclear Research Centre, <http://www.sckcen.be/>.

⁶<http://www.bnl.gov/world/>.

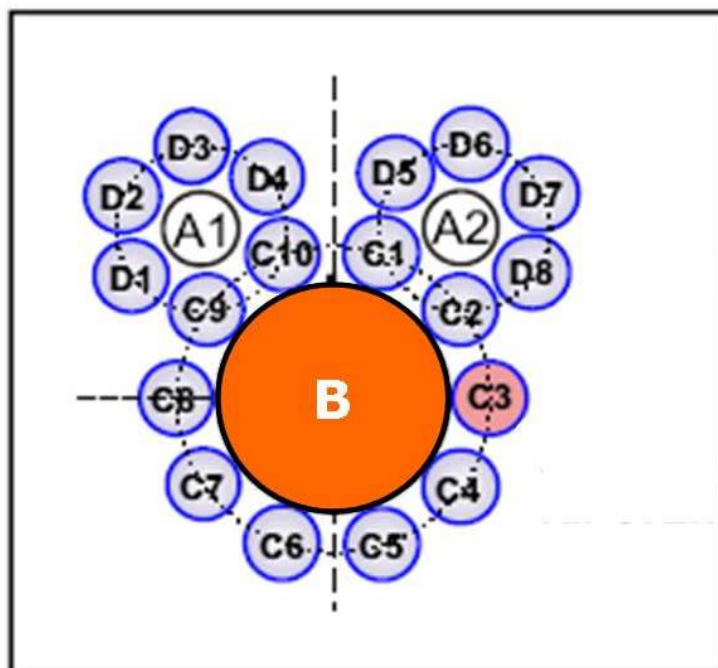


Figure 3. The picture above is a top-down schematic of the layout of the sources (labeled ‘C’) and the BRIGITTE exposure area, labelled B. The container of items to be exposed is lowered into the cavity labeled ‘B’ where the rods of ^{60}Co permit a near-uniform exposure.

1.01 kGy(Si)/hr uniformly throughout a volume 40 cm in diameter and 60 cm in height. Brigitte is located within a water tank containing one of the small test reactors while Rita is within a water tank outside the reactor. Both tanks are 8 m deep to provide shielding.

The sources are in the form of cylindrical rods which are themselves arrayed upright in a cylindrical shell and submerged 8 m in their respective water tanks. Shown in figure 3 is a top-down view of the configuration of source rods that surround the area where the vessel is lowered during exposure in Brigitte. A slightly buoyant, water-tight vessel can then be packed with material for exposure and lowered into the centre of the cylindrical shell of rods (see figure 4 for a side view of this vessel). In both cases the items under test were enclosed within the vessel allowing access to the devices through sealed tubing so that in-situ measurements could be performed throughout the radiation exposure. A similar configuration is arranged for the Rita exposure area. A description of the test configuration for the fibres is given in section 4.3.

The dose rate was measured using Red Perspex.⁷ These perspex squares were exposed for two hours in Brigitte and 24–48 hours in the RITA source. The dose measurement itself has a 3% uncertainty but precise location of the squares within the vessel limits the total uncertainty to $\pm 5\%$ on the absolute dose measurement. The dosimeters were in water, therefore a correction was applied, in order to obtain the dose rate for Si. The correction factor was calculated from the X-ray mass absorption coefficients for silicon and water⁸ and this correction decreased the doses by 11%.

⁷Red Perspex Type 4034, Harwell, <http://www.harwell-dosimeters.co.uk/specifications>.

⁸<http://physics.nist.gov/PhysRefData/XrayMassCoef/tab3.html>.

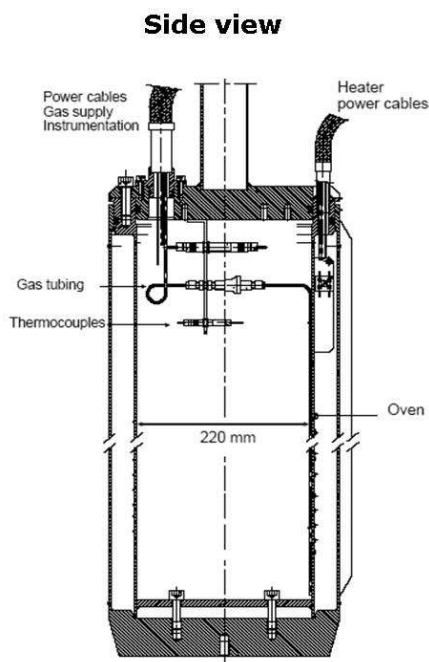


Figure 4. Shown is a drawing of the water-tight vessel used in Brigitte to contain the experimental apparatus. A similar vessel was used in Rita. The full height of the vessel (dimension not shown) is approximately 1 meter and the maximum radiation dose is delivered to a 10 cm height approximately 20 cm from the bottom of the vessel.

Table 4. Measured doses in water for different depths measured from the top of the Brigitte vessel, using two hour exposures.

Depth (mm)	Dose kGy(H ₂ O)
685	9.7
835	22.9
985	43.2
1095	51.5
1095	50.3
1135	50.5
1135	49.6
1175	48.5
1175	47.1

Table 4 shows the radiation dose as one measures downward from the top of the vessel when it is fully lowered within the source, for Brigitte. A volume profile was not considered necessary for Rita as it had been previously shown to have a high degree of uniformity. The delay between the dose rate readings being taken and the exposure was short, so the correction for the half-life of ⁶⁰Co was negligible.

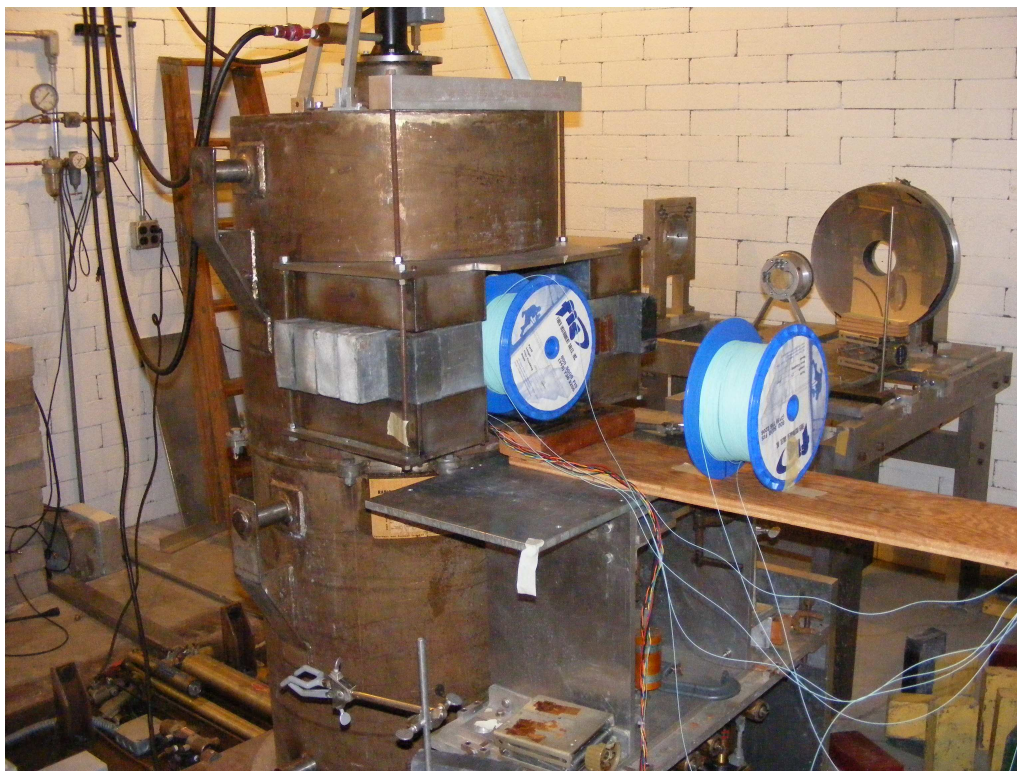


Figure 5. Picture of the radiation set-up at BNL. The ^{60}Co source is located behind the lead shielding blocks on the left. Two spools of fibres can be seen at different distances from the source and are therefore receiving different dose rates.

4.2 The radiation facility at BNL

The BNL Solid State Gamma-Ray Irradiation Facility is inside the Brookhaven National Laboratory, Upton New York. The facility contains a 2500 Curie ^{60}Co radiation source located in a dedicated room (irradiation chamber). All irradiations are made in air at distances from 10 cm – 100 cm away from the source. The source provides a maximum 0.4 kGy(Si)/hr dose at the 20 cm by 20 cm window of the source container (see figure 5).

Different dose rates can be obtained by placing the sample at different distances away from the window. For small samples that can be placed inside the window, higher dose rates can be achieved. When the source is lowered into its cylindrical container, people can enter the chamber to set up samples and connect readout cables. Test equipment is usually placed in an area about 15 meters away from the source. Connection cables are routed in a cable tray from the chamber to this area. There is no volume limit on the cables to be used. The equipment can be accessed by people for monitoring and data logging while the samples are irradiated. There is no temperature and humidity control for the chamber other than a normal air conditioning unit to keep the environment to about 25 °C.

The dose rate is measured using LiF thermoluminescent dosimeters (TLDs).⁹ Each TLD is a single small calibrated LiF crystal enclosed in a small plastic bag irradiated at the position to be determined for a known period of time. The overall error is estimated at $\pm 10\%$.

⁹Service provided by Landauer Inc. <http://www.landauerinc.com/>.

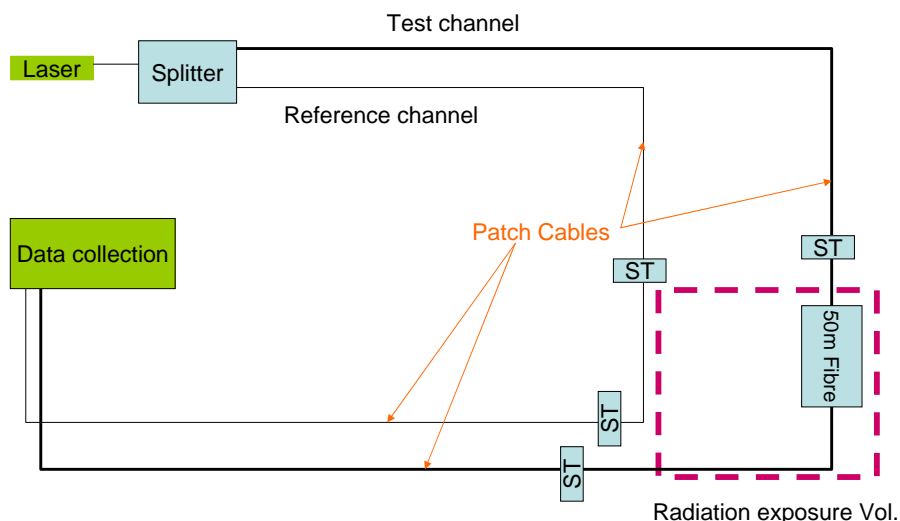


Figure 6. The drawing above is a schematic diagram of the test system used to measure the radiation damage of all our optical fibres. In all cases at least 30 m of fibre were coiled within the radiation environment so that the radiation level was uniform across the full length of fibre. Each channel's light levels were recorded by a *p-i-n* diode connected to an integrating amplifier. This test system was used in all radiation environments reported within this paper. ST refers to ST optical connectors.

4.3 The experimental configuration

The experimental system for all tests is relatively simple and a description of the system for a single channel follows. Test systems based on the principles described here were used in all the tests. In a remote, radiation-free location the light from a laser is launched down an optical patch cable. The laser signal is first split via an optical splitter and the light sent to the exposure vessel through a further long length (many metres) of patch cables. A connection to the fibre under test is made at the top of the vessel and the equal-length return path brings the light from the fibre under test back to the remote area where it is converted to an electrical signal by a *p-i-n* diode and amplified. The lasers are operated continuously and with DC light levels. A block diagram illustrating the above description is shown in figure 6.

The radiation induced absorption (RIA) is obtained by measuring the ratio of light returned from the test channel to that from the reference channel.

In both exposure vessels at SCK-CEN the radiation levels just outside the main exposure area are orders of magnitude less strong, but still represent a measurable component of the full damage. The experimental system is devised to correct for any damage of the patch cables. Consequently, one light path from the optical splitter goes to a short (1–2 m) length of fibre which is near the top of the vessel. This ensures that the measured damage is only from the fibre under test.

The laser light is split because all lasers, unless carefully controlled with temperature and optical feedback circuitry, tend to have long-term stability issues regarding their light output. Splitting the laser light allowed any intensity instabilities that occur not to effect the relative strength of the returning signals from the fibre under test and its reference. However, this system cannot provide any protection against changes in laser modes which can affect the splitter power ratio. At

SCK-CEN the lasers were all driven by hard current sources which, according to our own tests, had better than one part in one thousand temperature stability over a range of 100°C. VCSEL's from TrueLight^{tm10} and edge-emitting laser diodes (EEL)¹¹ provided the 850 nm and 1310 nm sources respectively.

The light signal from each channel is received via *p-i-n* diodes. The circuit used is simply to place the diode in series with a precision, temperature-stable resistor and reverse bias the combination with 12 Volts from the VME crate power supply. Each channel has high frequency bypass capacitors located close to the diodes to provide power supply noise isolation. The current through the diode is sensed by the voltage across the precision 3.3 kΩ resistors which was sent across a dedicated backplane to a series of integrating amplifiers. These digitise the signals and present the results to the standard VME interface for readout through the VME controller to a laptop computer. The coordination of readout and data collection is controlled via the laptop computer using LabViewtm.

Each amplification channel was checked for stability, dynamic range, and linearity. This was done by using a DC power source connected to a resistor chain made of precision resistors with an absolute value measured to 100 ppm and a ratio between any two devices to better than 10 ppm. The results indicated a degree of linearity and stability to approximately 100 ppm which is well below the stability available to us from the laser sources used. Tests were also performed using Light Emitting Diode (LED) sources confirming this level of stability over extended time periods of up to 70 hours of continuous operation. Consequently, we are confident that the degree of instability seen in our laser tests is due entirely to the coupling efficiency of the lasers alone. In normal operation we take a reading from all channels once every 10 seconds. The results are stored in a text file for later analysis.

Slight variations were discovered in the pedestal (zero value) of the amplifiers when a dark signal was on the *p-i-n* diodes over the course of extended runs. We removed this effect by taking a dark measurement prior to and after every test run. The pedestal used is interpolated between these readings for each channel. These corrections were applied throughout the paper. The magnitude of the variations in the pedestals were equivalent to much less than 0.1% of the signal and hence the resulting uncertainty was a negligible effect in comparison to other sources of systematic error.

At BNL an equivalent system was used to measure the RIA during the radiation exposure. In this case single channel VCSELs¹² were used.

4.3.1 The Brigitte (high dose rate) experiment

Next we describe the specific details of this particular test in the high dose environment. All five fibres were under test using laser sources. Each laser channel was split using fused taper 1x4 splitters, where one channel of each splitter acted as the reference channel for that splitter. The three Draka fibres shared the same reference. The Infinicor SX+ and the SMF-28 fibres each used their own reference on different splitters.

All of the channels returned between 100 μW and 300 μW of optical power as measured by an optical power meter prior to radiation exposure and before coupling into the *p-i-n* diodes. This can only be seen as a rough power estimate, as disturbing the fibres in any way could cause fluctuations in the transmitted power by up to 50%.

¹⁰Truelight TSA-8B12-00, <http://www.truelight.com.tw/>.

¹¹Iflatel UCF:V-FPT 13b-R4202.

¹²VCSEL of the same type as used by the ATLAS LAr OTx.

In order to obtain a full dose equivalent to at least that of the SLHC application, the initial exposure was for approximately 32 hours at 22.5 kGy(Si)/hr. All of the fibres under test were exposed to this level of gamma radiation. The entire 50 m length of each fibre under test was coiled around teflon spools confined within the 10 cm depth of highest exposure. The spools were held in place by aluminium disks bolted to a gantry within the watertight vessel. In addition to recording the returning light levels, the temperature of the spools holding the fibre was monitored with a thermocouple. The temperature of the remote crate containing the laser sources was also monitored. As will be seen in later sections, in Brigitte the radiation levels are so high that significant heating occurs within the vessel from Compton scattering.

After the initial 32 hours of exposure, the vessel was lifted out of the exposure area but left within the water tank for approximately 12 hours in order to observe any annealing effects after exposure. The lasers continued to be operated during this period. After the annealing period we returned the vessel to the exposure area for a further exposure (approximately 6 hours) before permanently removing the system from the site.

4.3.2 The Rita (low dose rate) experiment

We exposed two 50 m lengths of the Infinicor SX+ fibre in the Rita vessel concurrently with our exposures at Brigitte. One length was illuminated using a single VCSEL from an array while the other used an LED source. The VCSEL illuminated fibre provided a direct comparison to the similarly illuminated fibre in the high dose experiment and showed the differing effects of temperature and exposure rate on the same optical fibre. The LED illuminated fibre used light levels in the range 1–3 μ W, which is two orders of magnitude lower than used for the VCSEL illuminated fibre. Since the fibre for the two tests came from the same reel and all other conditions were identical, a comparison of the RIA from the two tests is sensitive to the effects of photo-bleaching.

A similar test was not performed on the SMF-28 fibre because we anticipated this fibre would be exceptionally radiation hard at even the highest doses. We therefore did not expect further study of the single mode fibre would be required (and as we shall show, these predictions were justified).

4.3.3 The BNL experiment

The BNL facility was used to expose the Infinicor SX+ fibre to three different dose rates (see table 3). For the BNL tests the fibres under test was in a protective jacketing consisting of a tight buffer with an outer diameter of 0.9 mm. Different jacketing might have an impact on the stress experienced by the wound fibre and hence on its mode distribution. If the jacket degrades significantly with radiation this might change the stress on the fibre and hence the mode distribution. This is different to the situation for the SCK-CEN tests, which used bare fibres (ie the fibres had a primary acrylate layer but no plastic buffer). At the low dose rates used for these tests, no significant radiation induced heating would be expected. The irradiation was continuous apart from short interruptions. The monitoring of the RIA was continued for a short time after the fibres were removed from the radiation zone in order to observe any annealing.

4.3.4 Stability tests and experimental accuracy

Prior to the radiation exposure we performed long-term tests of the stability of the two systems used at SCK, complete with patch cables, fibres under test, and their references. The system was

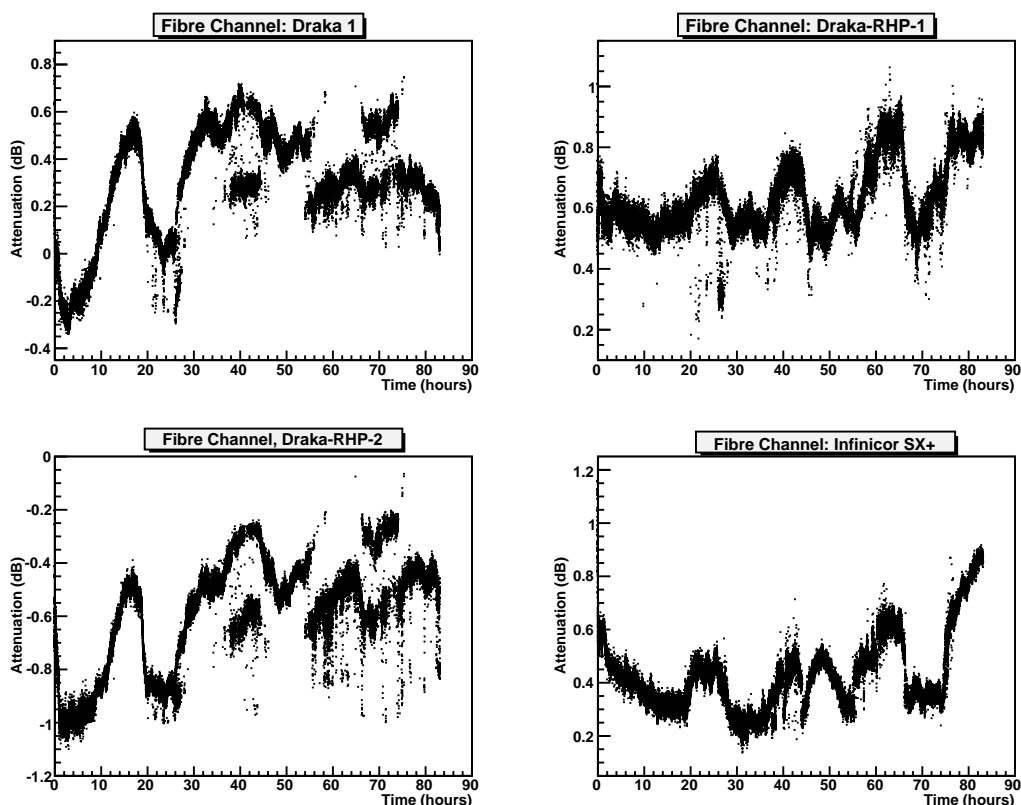


Figure 7. Shown above are plots of the light levels from each fibre channel relative to its reference prior to exposure to radiation. Places where it appears the result is not single-valued are simply an artifact of taking a reading every 10 seconds on this scale. If the measurement of a channel flips between two discrete values on a random timescale of a minute it would appear on this scale to have two distinct values at once even though it does not.

left to run for approximately a week (spanning $\simeq 80$ hours) at the end of July 2008. Both laser and LED sources were running and both the high and low dose test systems were operational. Dark pedestals were recorded both before and after the run period and subtracted from the results.

Figure 7 shows the results of our stability tests over a long run of greater than 80 hours with the full experimental system. Several such tests were done and the results were all similar to these which are here shown. Figure 7 shows the light output in decibels relative to the reference channel. As 50 m of fibre were used for all the tests, the fluctuations visible in this plot will be divided by a factor of 50 when measuring the RIA in units of dB/m.

For the SCK tests the RMS stability for each of the 4 multimode fibres was less than 0.25 dB. Therefore, when divided by the lengths of our fibres under test this translates to a systematic uncertainty on the RIA of ± 0.005 dB/m. A similar analysis for the BNL set-up immediately prior to irradiation indicated that the systematic uncertainty on the RIA was less than 0.002 dB/m. The equivalent analysis for the SM fibre yields a systematic uncertainty of ± 0.0005 dB/m, which is an order of magnitude better than for the multimode fibres.

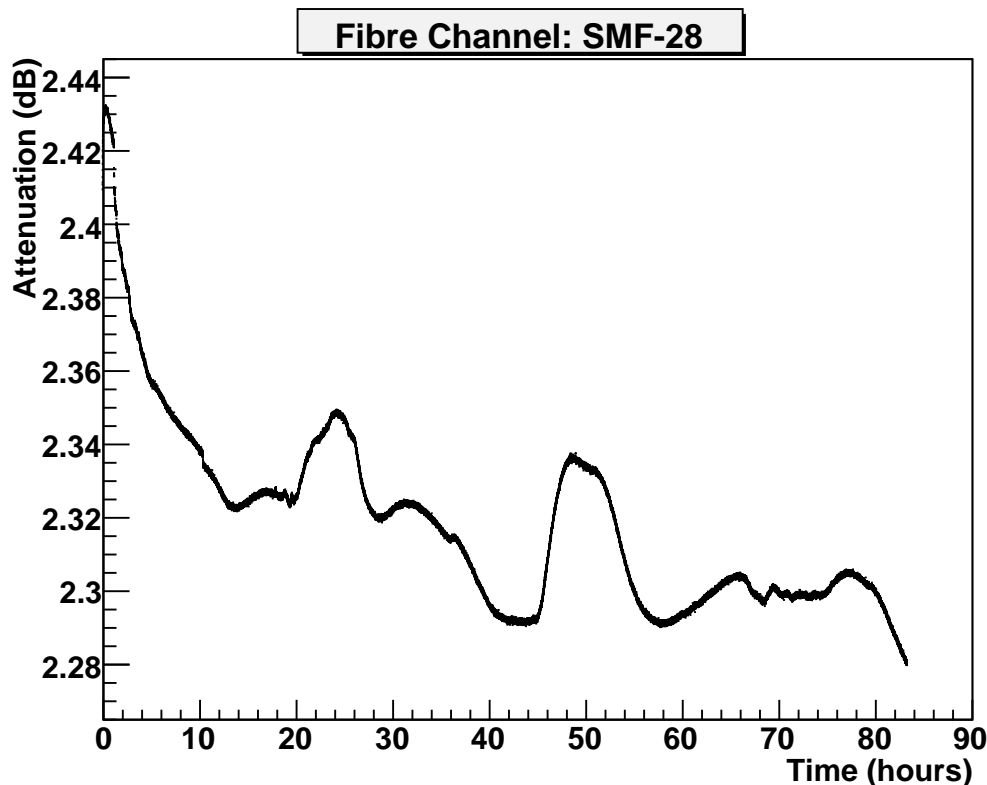


Figure 8. Light level relative to its reference as a function of time prior to radiation for the SMF-28 single-mode fibre.

4.3.5 Further discussion of the stability of the multimode system

As the reader can see from the stability plots presented, there are stretches of time when a given channel achieves a stability far superior to the long term value of ± 0.005 dB/m: However one cannot anticipate those times when significant instabilities at the level of a quarter decibel will arise. The effects are uncorrelated with any temperature variations and are not related to variations in the current supplied to the laser diodes. We believe that these fluctuations are due to laser "mode hopping" which cause changes in the transverse modes coupled into the fibre. The fact that the stability of the LED tests was far superior to that of the VCSEL tests (see figure 12), provides some evidence for this hypothesis because the LED source fills the transverse modes of the fibre.

The stability of the relative attenuation for the single-mode fibre is shown in figure 8. The variations are clearly much smaller than for the multimode systems using VCSELs. This observation is also consistent with the mode-hopping being the cause of the instability in the multimode system, as the mode stability of EELs are expected to be better than VCSELs. However, the majority of the tests for multimode fibres were performed with VCSELs rather than LEDs as these gave more realistic optical power for LHC experiments and this is important for photo-bleaching (see section 5.2).

We are currently studying various ways to improve the stability of our multimode system for future measurements. However, by using 50 m of fibre we were able to mitigate these inherent uncertainties and obtain results of sufficient quality for our purposes.

5 Test results

This section gives the experimental results from the different radiation sources. The results for the Infinicor SX+ fibre from the different sources are combined in order to understand the effect of varying dose rates. The data is then used to evaluate the expected RIA that would be expected for a plausible fibre routing for the ATLAS tracker at SLHC. Possible causes of the high spike in attenuation experienced shortly after immersion in the radiation field are discussed and proposals for future tests are given.

5.1 High dose results — Brigitte

In order to study annealing effects, the Brigitte vessel was lifted out of the radiation area for several hours and then re-inserted for a further 5 hours before final removal. All of these timescales are visible on a plot of relative attenuation vs. time for all of the fibres tested as shown for example for the SMF-28 fibre in figure 9. The plot shows a very sharp increase in RIA at the start of irradiation (a). The RIA quickly reaches a maximum (b) and then decreases to a minimum (c). After this the RIA increases monotonically with time (d) until the vessel was removed from the radiation. The RIA then appears to show significant annealing (e). However this annealing disappears very quickly when the vessel is returned to the radiation zone and a similar spike in RIA is observed as at the start of the second irradiation. These qualitative features were observed for all the types of fibres exposed at the highest dose rate. Similar results have been seen in previous work, see for example [10]. Therefore, care has to be taken not to overestimate the annealing effects, when predicting the RIA for a particular scenario (see Section 5.4.1). The very rapid initial increase in RIA will be more completely discussed in Section 5.5.

The measured dose rate was used in combination with the data shown in figures 9 to generate a plot showing the RIA of the SMF-28 fibre as a function of the total dose (see figure 10).

An equivalent procedure was used to generate the plots of RIA versus dose for the four types of multimode fibres and the results are shown in figure 11.

5.2 Intermediate dose rate results — Rita

The Infinicor SX+ fibre was exposed for approximately 70 hours in the Rita facility at a dose rate of 1.01 kGy(Si)/hour (a factor of ~ 25 less intense than those experienced within the Brigitte vessel). The results of these tests are shown in figure 12. Within the lower dose vessel (Rita) there were two different intensities of light passed through equivalent lengths of this fibre which had come from the same preform in the manufacturing process. One length was transporting $\approx 100 \mu\text{W}$ from a VCSEL source while the other was transporting $\approx 1 \mu\text{W}$ from a light emitting diode source (LED). The results of both tests are shown in figure 12. The RIA for the Infinicor SX+ fibre illuminated with a VCSEL (LED) reaches a value of 0.06 dB/m (0.13 dB/m) at the end of the irradiation (see figure 12). This significant difference shows clear evidence of the impact of photo-bleaching, since the exposure environment was identical in both cases.

5.3 Low dose rate results BNL

The RIA versus dose for the three different dose rates for the Infinicor SX+ fibre are shown in figure 13. The measured RIA for the same dose increases with increasing dose rate. This is expected,

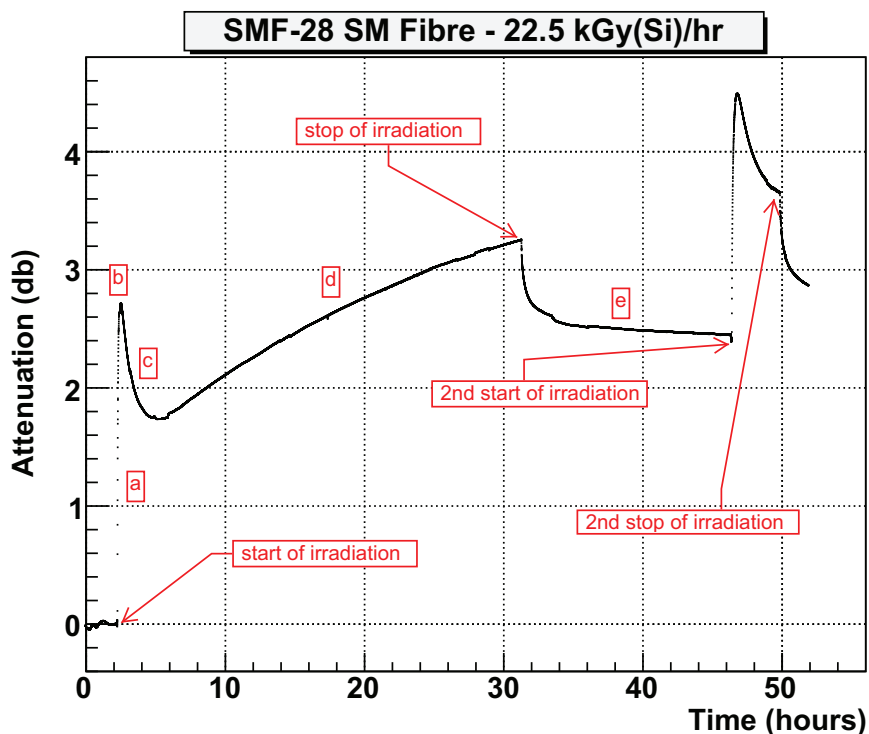


Figure 9. Total attenuation of the 50 m length of SMF-28 single-mode fibre vs. time to the end of the full run at SCK-CEN. Note that the vertical axis is in dB. See text for further explanation.

as lower dose-rate radiation allows a longer time for annealing for the same total dose. There were some short interruptions to the exposure which can be seen as the dips in the RIA. It is interesting to note that after the exposure resumed, the RIA came back to the level that would have been expected from before the break in the exposure. This confirms the similar effects seen in the SCK data for all fibre types. The most plausible explanation for this effect is that after the end of the irradiation, photo-bleaching removes the electrons from the trap sites whilst leaving the traps in place. After the irradiation is resumed, the trap sites are very quickly filled by electrons and hence the RIA returns to its previous value.

5.4 Combined results

All of the results for the Infinicor SX+ fibre are shown in figure 14 which shows clear evidence of dose rate effects; within a given facility the damage for a given dose increases monotonically with dose rate. However, the data from the lowest dose rate at SCK (Rita) overlaps with even lower dose rates measured at the BNL facility. This apparent discrepancy is compatible with each test's systematic uncertainties (see section 4.3.4).

5.4.1 Route specific RIA

This data discussed so far are valuable but do not, for us, answer the central question as to whether or not this damage would be acceptable or unacceptable for use in a specific physics experiment at the SLHC. As the fibre routing takes the signals out of the detector through long runs in relatively

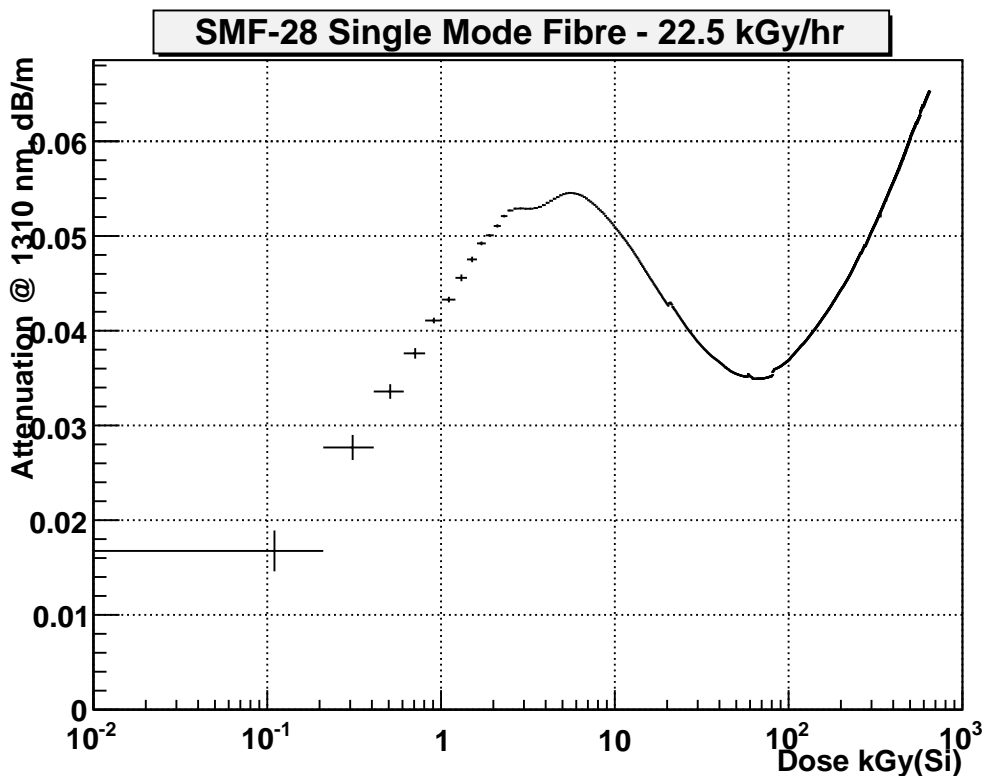


Figure 10. RIA of the SMF-28 single-mode fibre vs. dose at SCK-CEN up to the end of the first stop of irradiation (see figure 8). Note that the vertical axis is in dB/m. See text for further explanation.

low radiation areas it could be that our optical signal will still be significantly degraded due to the attenuation acquired by the fibres at low doses as well as that due to the shorter runs in the high radiation area close to the detector.

Since the RIA increases with dose rate and all the radiation tests were performed at higher dose rates than expected at SLHC, it is possible to estimate a conservative upper limit on the RIA that would be expected at SLHC by combining the data at the different dose rates. Since the dose rates used in this study were much higher than that expected at SLHC, and the data show evidence for very significant dose-rate effects, this procedure will result in a very conservative upper limit for the expected RIA.

To understand better what these results mean for a given typical routing scheme we used our data for the Infinicor SX+ fibre and parametrised its behaviour to radiation damage. The curve fit to radiation damage was done in sections and based entirely upon the data collected by the tests shown in figure 14. Since the dose rates expected at the SLHC will be lower than any of those used in these tests, the curve explicitly ignores the high-level attenuation spike in the highest dose-rate data in favour of the lower rate studies up until a dose of 170 kGy(Si). The curve is shown with the data used in figure 14. The functions used are described in detail in appendix A. Then a model of the fibre route out of the ATLAS detector was employed to estimate the total attenuation that one might expect from a worst-case routing of this fibre starting from a location 30 cm distant in radius from the interaction region (see table 5).

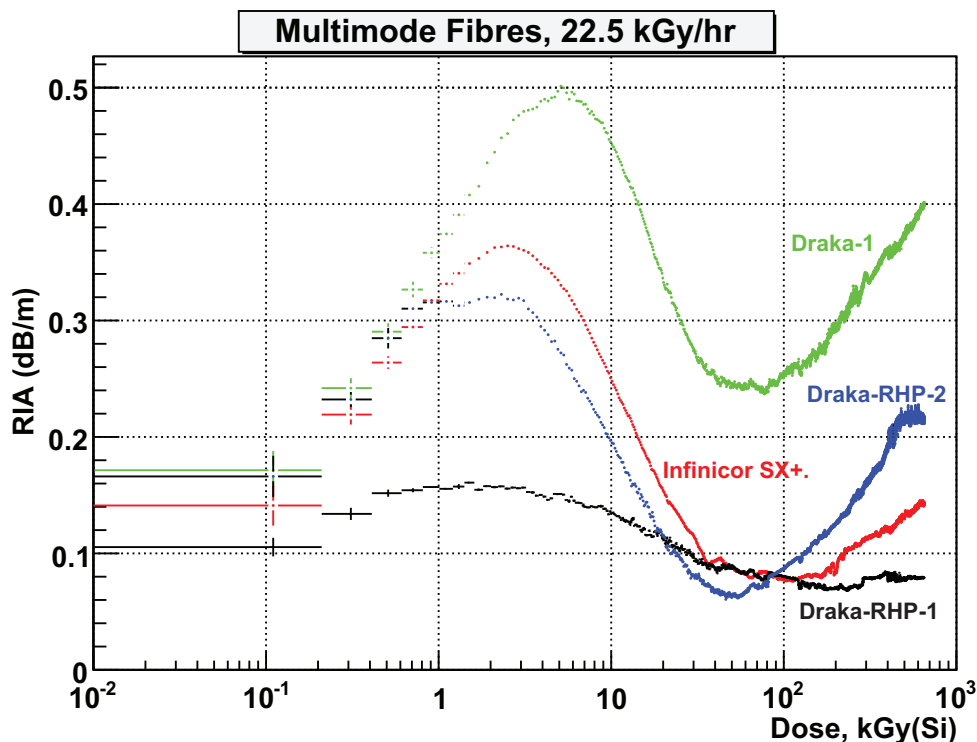


Figure 11. This plot shows the RIA obtained as a function of integrated dose for the four multimode fibres tested at a dose rate of 22.5 kGy(Si)/hour. The green curve is for Draka-1, the red curve is the Infinicor SX+. The black and blue curves are for Draka-RHP-1 and Draka RHP-2 respectively.

Table 5 lists the route chosen showing the lengths of fibre in each part. The route begins 30 cm radially from the beamline and 100 cm from the centre of the detector. Each “step” in the table represents one section of the route as the fibre snakes its way to outside of the radiation zone. The table also shows along each step the total length of fibre involved and an estimate of the radiation damage the Infinicor SX+ fibre would take given the levels of dose expected shown in figure 1 and using the parameterization shown in figure 14. Additional safety factors were applied in the calculation to take into account the uncertainties in the expected radiation doses. Inside the inner detector a factor of 1.5 was used. Outside the inner detector, the dose calculations are much more difficult because they are sensitive to details of the detector geometry, so a safety factor of 5 was used. Adding up the total damage after the full period of expected running in the upgraded LHC we obtain the result of 0.41 dB of total loss. It is interesting to note that most of the damage occurs for the longer runs of the fibre at lower doses, rather than the short run at high dose near the beam line. This calculation assumed conservative safety factors for the assumed dose. The calculation is also conservative in that it used data from higher dose rates than expected at the SLHC and no corrections were made for dose rate effects. Three remaining sources of systematic error were considered: dosimetry, RIA measurement accuracy and the fit functions used. The estimated systematic uncertainties are summarised in table 6. The final result for the estimated RIA for the Infinicor SX+ fibre in the ATLAS tracker at SLHC is 0.41 ± 0.05 dB. Although the final power budget for the optical links for SLHC applications has not yet been specified, this fibre is a suitable candidate use at SLHC for warm operation.

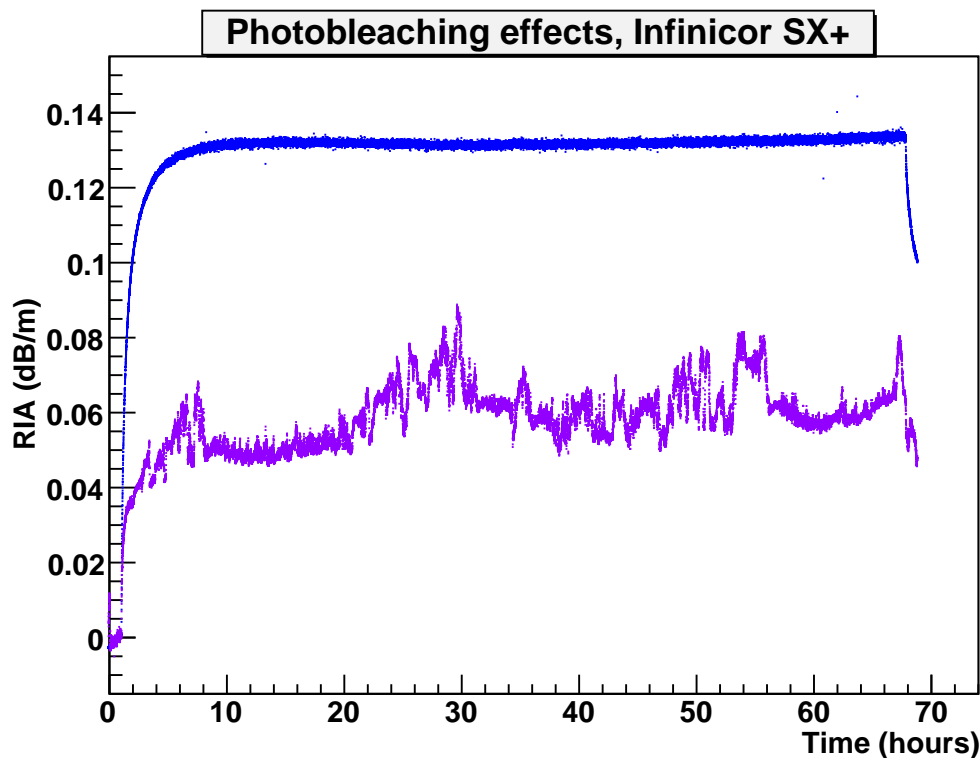


Figure 12. Shown is the effect on RIA of increasing the optical power on the same fibre subjected to radiation damage. The lower curve results from launching approximately $100 \mu\text{W}$ of laser power at 850 nm down the fibre while the upper plot used approximately $1 \mu\text{W}$ from an LED source with the same centre wavelength. Note the increased stability from the LED source, where a very large number of modes propagate down the fibre.

From the high dose rate measurements, the RIA for the Draka-RHP-1 and the SMF-28 fibres are less than that for the Infinicor SX+ fibre and would therefore be expected to have an even lower RIA for the assumed ATLAS operation at SLHC.

5.5 The early attenuation spike

All the high dose rate exposures show a feature of very rapid attenuation occurring almost instantaneously with immersion in the high-dose ^{60}Co source followed by a somewhat less rapid *decrease* in attenuation (see for example figures 9 and 11). The effect appears on all of the exposed fibres to some degree. Comparison to figure 14 of the Infinicor SX+ fibre shows that this effect is not present in any of our lower dose-rate tests done at SCK-CEN or BNL and we have no reason to suspect that, had the other fibre types been tested at low dose rate, the effect would have appeared.

In addition, as shown in figure 9 the effect re-appears after the initial exposure when the Brigitte vessel was briefly returned to the radiation environment. Though not shown, this feature appears in all the other fibre high dose rate tests as well. We conclude the process causing this attenuation spike is, to lowest order, a reversible process.

We are currently uncertain as to the exact cause of the fast attenuation and then rapid recovery but we have strong suspicions that it is related to the vessel temperature in the Brigitte facility cou-

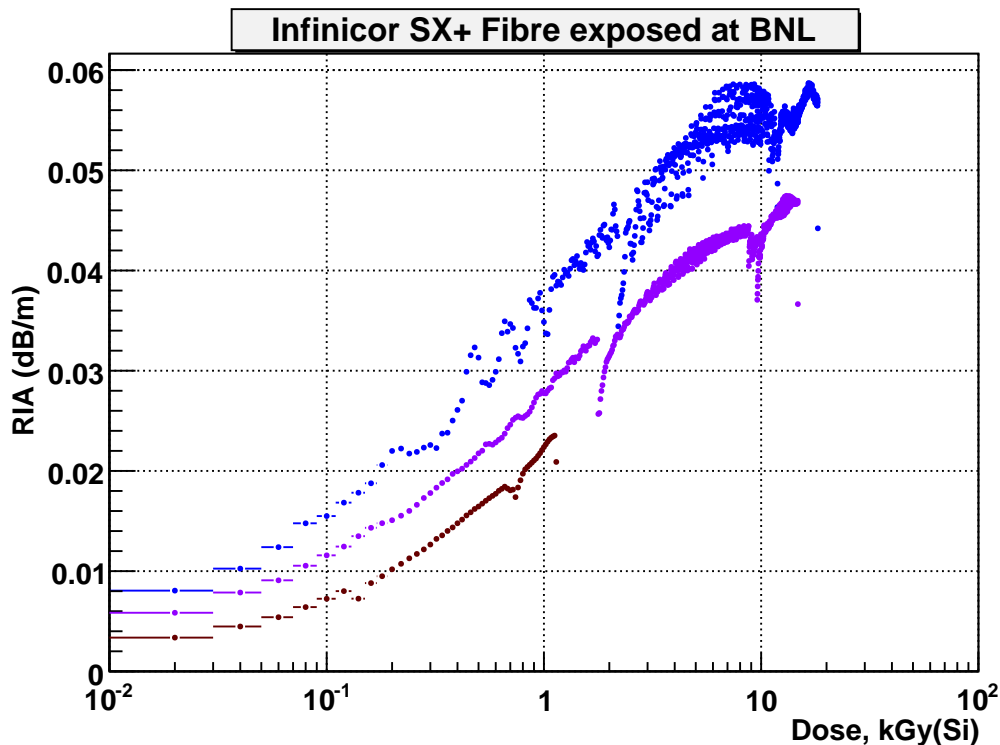


Figure 13. The RIA versus dose for the 3 different dose rates from the BNL data for the Infinicor SX+ fibre. The dark blue curve is for a dose rate of 0.424 kGy(Si)/hour and the light purple and brown curves are for dose rates of 0.343 and 0.0265 kGy(Si)/hour respectively.

Table 5. Expected RIA for the Infinicor SX+ fibre for SLHC, assuming a given fibre routing and using the fit shown in figure 13. All dimensions in ‘ r ’ and ‘ z ’ are referenced from the beamline and the centre of the ATLAS detector in a cylindrical coordinate system.

Step	ATLAS Fibre Route (cm)				Length	Loss (dB)
	r_{start}	r_{end}	z_{start}	z_{end}		
1	30	110	100	100	80	0.072
2	110	110	100	340	240	0.168
3	110	420	340	340	310	0.130
4	420	420	340	0	340	0.006
5	420	572	0	0	152	0.002
6	circum. step – $r = 572$ cm; $\Delta\phi = \pi$ radians				1797	0.023
7	572	1200	0	0	628	0.005
Total					35.5 m	0.407

pled with the known natural annealing behaviour of optical fibres. The fibres in Brigitte were held in place by solid aluminium disks of a diameter of 220 mm and an average thickness of 10 mm. Three such disks were used. Gamma ray photons at the energy of ^{60}Co decay will Compton scatter off the electrons in any material. In each such scattering energy is deposited in the material. If the flux of gamma rays is high enough this energy will eventually manifest as a measurable source of heat.

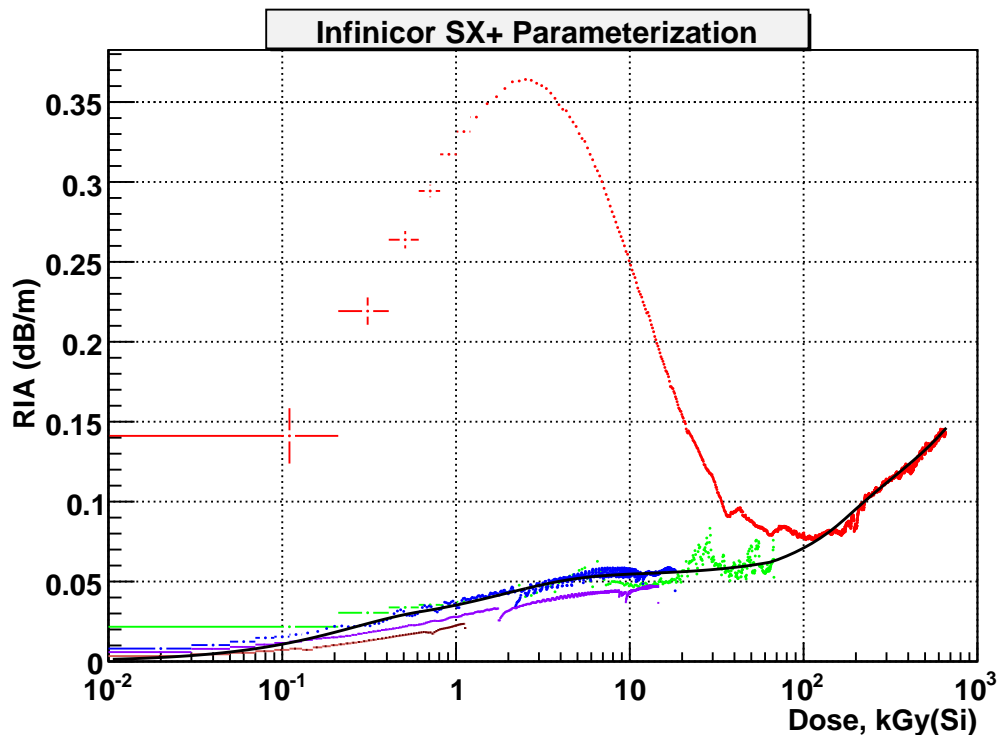


Figure 14. These plots show the RIA as a function of integrated dose for the Infinitor SX+ fibre. These are the same plots as the previous figure but shown on the same scale. The red curve is for a dose rate of 22.5 kGy(Si)/hour (Brigitte), the green curve for a dose rate of 1.01 kGy(Si)/hour (Rita) and the dark blue, light blue and green curves are from BNL at dose rates of 0.48, 0.38 and 0.026 kGy(Si)/hour, respectively. The continuous line is a result of a fit (see text).

Table 6. Systematic errors in the calculation of the route specific RIA.

Uncertainty	Systematic Error (dB)
Dosimetry	0.015
RIA measurement	0.05
Fit function used	0.009
Total	0.053

The Compton Scattering effect was certainly present in the Brigitte test. Figure 15 shows the full temperature measurements vs. time that were recorded within the vessel during exposure. One can see the programme of initial immersion for the SLHC-level test and then re-immersion in the temperature plot where the temperature within the vessel stabilizes near 70 °C, with approximately a 30 minute time constant. Figure 16 focuses in on the initial exposure and compares the four multimode fibre attenuation data to the temperature profile of the vessel. This plot shows that the initial fast rise in attenuation occurs on the timescale of about 1 minute, and, therefore the corresponding temperature change is less than 1 °C. This implies that the initial sharp rise in RIA cannot be due to a change in temperature. However, the temperature has risen by about 5 °C when

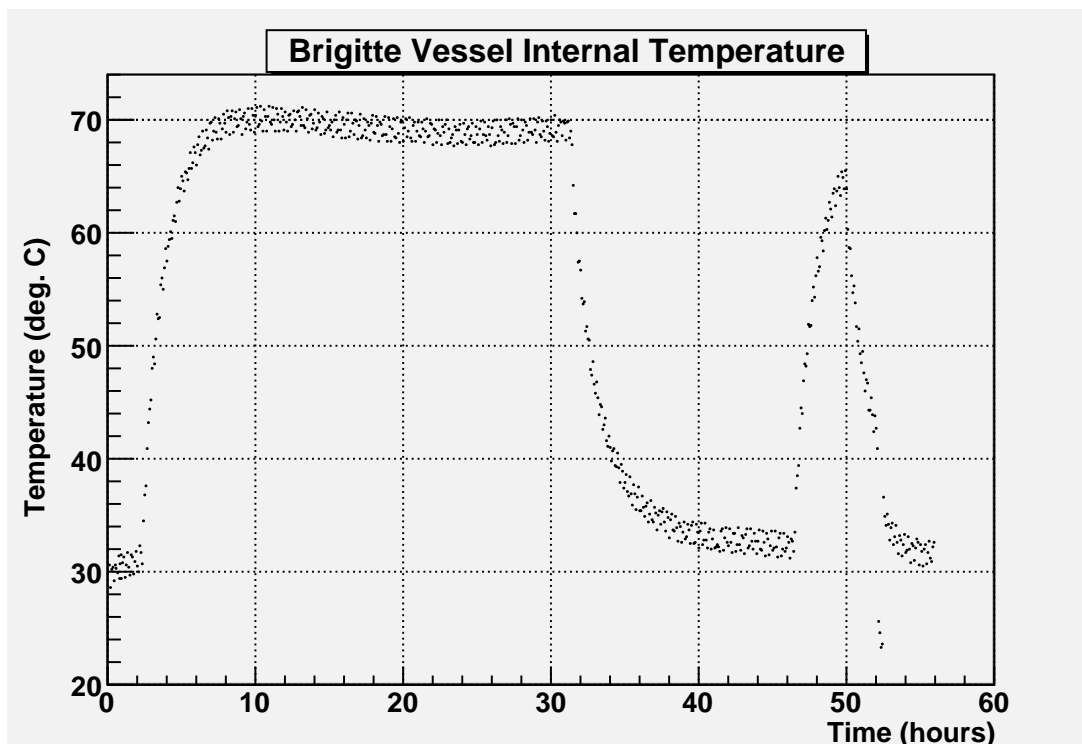


Figure 15. Plot of the temperature within the Brigitte vessel as a function of time. The first rise in temperature is when the vessel was first lowered into the radiation area. The decrease occurs after the vessel was removed for several hours to study photobleaching effects. The final temperature increase was due to a second exposure before the end of data taking.

the RIA starts to decrease. It is therefore possible that this decrease is related to the increase in temperature. It is very interesting to note that the one multimode fibre that has F dopant in the core (Draka RHP-1) shows a much smaller initial spike than the other multimode fibres that use Ge dopant in the core.

Similar effects have been observed in other experiments with optical fibres at high dose rates. For example, very strong transient absorption in the region around 700 nm has been observed and attributed to self-trapped holes (STH) [14], [15]. The explanation given is that the initial observed quick rise in attenuation is due to the presence of pre-existing defects within the fibre that naturally arise in any manufacturing process. In this case STH in the glass matrix are identified as the likely cause. STH put trap sites in the band gap between the conduction and valence band and a large influx of radiation will quickly fill those trap sites with electrons which will act as scattering centres for optical transmission. The effect is most pronounced in the visible region of the spectrum but has a continuum which extends well into the infrared. The fact that the relative peak size is significantly higher in our 850 nm fibres than in our 1310 nm tests supports this point.

Optical fibres also have a strong annealing behaviour to ambient temperature [16], [17]. The temperature dependence in the case of the fibres presented in [16], [17] was quite strong, but because all but one of the fibres used in these tests are Ge doped we have reason to suspect they too will exhibit a strong temperature dependence. However, since the F doped fibre (Draka RHP-1) showed the smallest initial spike in attenuation, we would expect its RIA performance to be the least sensitive to a decrease in temperature.

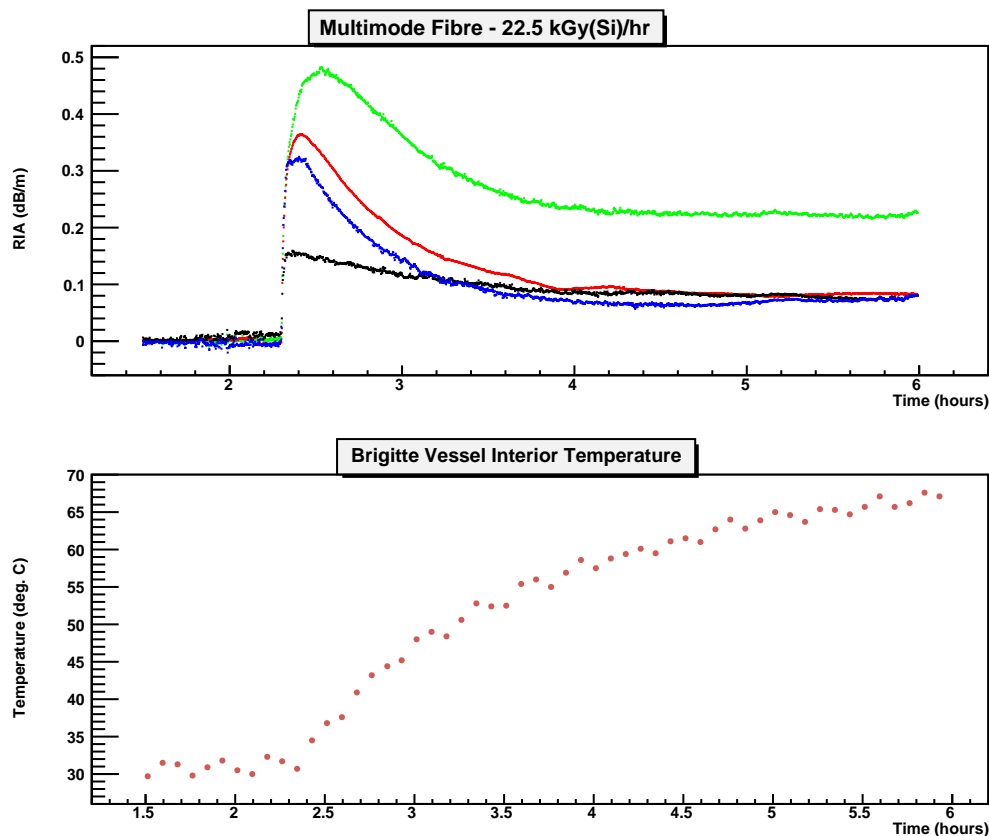


Figure 16. In this plot the RIA of all the multimode fibres under test in the high-dose area are shown vs. time but the time axis has been greatly expanded. Beneath this plot is the plot of the ambient temperature in the vessel containing these fibres plotted vs. time on the same scale.

As the temperature of the fibre increases, bonds that are associated with trap sites break, releasing the trapped electrons and improving the transmission characteristics of the optical fibre. We believe that we are seeing first the high attenuation caused by the immediate filling of trap sites from STH. These sites fill very quickly in a high-dose environment to a maximum that is reached within minutes of the exposure. In this particular case though, the temperature rise in the vessel was not far behind and as this temperature increased, the STH bonds were broken and the attenuation fell as a result. Radiation does, obviously, damage an optical fibre so this recovery period is limited both by the fact that the damage process continues and by the fact that the temperature profile does stabilize after two hours of exposure in this particular test (at around the 4.5 hour mark in figure 16). We believe the fact that a new minimum attenuation is reached at about this same time indicates that the temperature-annealing process is complete and the continuing damage from the gamma ray source takes over.

There is much that is still not well understood; however the LHC upgrade aspect of this experiment is concerned ultimately with dose rates on the order of 9 Gy/hr and since this effect only seems to occur at high dose rates it was ignored in the route specific calculation of the RIA calculations as discussed in 5.4.1.¹³

¹³This assumes 3 years of running with 10^7 seconds of operation per year and an integrated radiation dose at $r = 30$ cm and $z = 100$ cm of 250 kGy(Si) over 3 years of operation.

5.6 Future plans

Some parts of the path the fibre takes out of the upgraded LHC detectors might be in cold environments ($\sim -20^\circ\text{C}$). Since we observed strong temperature dependencies for the RIA, for a future study we intend to take further samples from our same Infinicor SX+ reel and repeat this test under both constant room temperature and temperatures approaching -20°C to determine the sensitivity of this fibre to temperature variations in a radiation environment.

Tests of the bandwidth of the fibres before and after irradiation will also be performed in order to determine if the radiation causes any significant degradation.

6 Conclusions

We subjected three Ge-doped multimode fibres, one F-doped multimode fibre and one single-mode fibre to gamma radiation at 22.5 kGy(Si)/hr to an integrated dose of 650 kGy(Si) . We also subjected the Infinicor SX+ fibre to several lower dose rates ($1.01, 0.424, 0.343, \text{ and } 0.0265\text{ kGy(Si)/hr}$) to study dose rate effects and provide data at low integrated doses. There is clear evidence that the damage is lower at the same dose for lower dose rates, which we ascribe to annealing effects. We have seen an apparent annealing after the end of irradiation but we have confirmed that the damage reappears almost immediately when the irradiation is restarted. From comparisons of irradiation of two samples of the same multimode fibre, performed under identical conditions, apart from the light levels, we conclude that there is clear evidence for photo-bleaching.

A curious spike in attenuation appeared in all fibres tested at the highest dose rate which is not yet completely understood. However we presented evidence supporting the hypothesis that variations in the temperature of the fibre's environment at the early stages of exposure contributed to this effect.

Two multimode fibres (Infinicor SX+ and the Draka-RHP-1) have been tested in various radiation environments and have been shown to exhibit sufficiently small losses through a typical routing from the ATLAS experiment for use in the upgraded LHC environment at or above room temperatures. One SM fibre (SMF-28) was also qualified for use in this environment. Under these conditions the Infinicor SX+ fibre had the largest RIA of the three fibres. A very conservative upper limit for the estimated total RIA for the Infinicor SX+ fibre, for a specific route to the ATLAS counting room, is 0.41 dB .

Acknowledgments

The Oxford group acknowledge financial support from the UK Science and Technology Facilities Council. The SMU group acknowledge the US-ATLAS R&D program for the upgrade of the LHC, and the US Department of Energy grant DE-FG02-04ER41299. This work was carried out in the context of the Versatile Link project [18]. The authors would like to thank Hans Ooms from SCK-CEN for a great deal of advice and help in the implementation and operation of this experiment. We would also like to thank SCK-CEN for providing the facility to carry out the tests. We would like to thank Benoit Brichard from SCK-CEN for his advice and information on optical fibre performance. We would also like to thank Francois Vasey and Jan Troska from CERN for their organisational help and critical assessments of our experimental proposals. Finally we must reserve special thanks to

Karl Gill from CERN who initially introduced us to the SCK-CEN facility and who has provided us with invaluable advice and help over several years. We thank M.-L. Chu and P.K. Teng for providing the VCSELs used at SCK.

A RIA fits functions

The fit functions used in the calculations for the RIA for the Infinicor SX+ fibre for a specific fibre routing in ATLAS are given below for the different ranges used. Here d is the dose in kGy(Si) and r is the RIA in units of dB/m. The data from the highest dose rate at BNL and from Rita are used for $d < 65$ kGy(Si). The data from Brigitte are used for the region $d > 170$ kGy(Si). A simple linear interpolation was used in between these two fits, in order not to be biased by the initial spike in the Brigitte data.

$$d < 0.6 \quad r = 0.03448 [1 - \exp(1 - d/0.2664)] \quad (\text{A.1})$$

$$0.6 < d < 65 \quad r = 0.03119 [1 - \exp(d/1.482)] + 0.02245 + 1.3510^{-4} d \quad (\text{A.2})$$

$$65 < d < 170 \quad r = 2.510^{-4} d + 0.04595 \quad (\text{A.3})$$

$$170 < d \quad r = 0.092393 [1 - \exp(-d/103.097)] + 8.1310^{-5} d \quad (\text{A.4})$$

References

- [1] N. Hessey, *Overview and Electronics Needs for ATLAS and CMS High Luminosity Upgrades*, in *Proceedings of the Topical Workshop on Electronics for Particle Physics*, Naxos, Greece, September 15–19 2008, [CERN-2008-008](#).
- [2] Joint ATLAS-CMS working group on optoelectronics for SLHC, K.K. Gan et al., *Report from sub-group B, Optical System Irradiation Guidelines*, EDMS Id 882783, available at <https://edms.cern.ch/document/882783/2.6>.
- [3] I. Dawson, private communication.
- [4] ATLAS radiation flux maps, http://atlas.web.cern.ch/Atlas/GROUPS/PHYSICS/RADIATION/Radiation_tables_jan03.html.
- [5] F. Berghams et al., *An Introduction to Radiation Effects on Optical Components and Fiber Optic Sensors*, Springer, Netherlands (2008), pg. 127–165 [ISBN: 978-1-4020-6950-5], http://dx.doi.org/10.1007/978-1-4020-6952-9_6.
- [6] B. Brichard et al., *Radiation Effect in Silica Fiber Exposed to Intense Mixed Neutron-Gamma Radiation Field*, *IEEE Trans. Nucl. Sci.* **48** (2001) 2069.
- [7] G. Mahout et al., *Irradiation studies of multimode optical fibres for use in ATLAS front-end links*, *Nucl. Instrum. Meth. A* **446** (2000) 426.
- [8] H. Hanafusa et al., *Drawing Condition dependence of radiation-induced loss in optical fibres*, *Electron. Lett.* **22** (1986) 106.
- [9] T. Wijnands et al., *Optical Absorption in Commercial Single Mode Optical Fibers in a High Energy Physics Radiation Field*, *IEEE Trans. Nucl. Sci.* **55** (2008) 2216.
- [10] H. Henschel et al., *A New Radiation Hard Optical Fiber for High-Dose Values*, *IEEE Trans. Nucl. Sci.* **49** (2002) 1432.

- [11] D.L. Griscom et al., *Radiation-Induced Defects in Glasses: Origin of Power-Law Dependence of Concentration on Dose*, *Phys. Rev. Lett.* **71** (1993) 1019.
- [12] J. Troska et al., *Radiation effects in commercial off-the-shelf single-mode optical fibres*, *Proc. SPIE* **3440** (1998) 112.
- [13] K. Gill, private communication.
- [14] D. Griscom, *Self-trapped holes in amorphous silicon dioxide*, *Phys. Rev.* **B 40** (1989) 4224.
- [15] D. Griscom, *Radiation hardening of pure-silica-core optical fibres: reduction of induced absorption bands associated with self-trapped holes*, *Appl. Phys. Lett.* **71** (1997) 175.
- [16] H. Kanamori et al., *Transmission Characteristics and Reliability of Pure Silica-Core Single-Mode Fibers*, *J. Lightwave Technol.* **4** (1986) 1144.
- [17] S. Thériault, *Radiation effects on COTS laser-optimized graded-index multimode fibers exposed to intense gamma radiation fields*, *Proc. SPIE* **6343** (2006) 63431Q.
- [18] L. Amaral et al., *The Versatile Link, A Common Project for Super-LHC*, in preparation, to be submitted to *JINST*.